Simultaneous Observation of Silicon and Boron Impurity Behaviors in the Core Region of a Mid-Density LHD Plasma

Naoki TAMURA[1,2], Mikirou YOSHINUMA[1], Katsumi IDA[1,2], Chihiro SUZUKI[1,2], Motoshi GOTO[1,2], Tetsutarou OISHI[1,2], Mamoru SHOJI[1], Kiyofumi MUKAI[1,2] and Hisamichi FUNABA[1]

[1]*National Institute for Fusion Science, National Institutes of Natural Sciences, 322-6 Oroshi-cho, Toki, Gifu 509-5292, Japan*

[2]*The Graduate University for Advanced Studies, SOKENDAI, 322-6 Oroshi-cho, Toki, Gifu 509-5292, Japan*

(Received 2 July 2021 / Accepted 18 July 2021)

Line emissions from both silicon (Si) and boron (B) impurity ions introduced by a single tracer-encapsulated solid pellet (TESPEL) containing silicon hexaboride (SiB_6) powders were successfully observed using the extreme ultraviolet (EUV) spectrometer and charge-exchange spectroscopy (CXS) technique in the Large Helical Device. The CXS diagnostic shows clearly that a hollow radial profile of fully ionized B impurities was created immediately after the TESPEL injection, and such a hollow profile was relaxed with time. At the same time, Li-like emissions from the highly ionized Si impurities were also observed with the EUV spectrometer, SOXMOS. Therefore, the decay times of these impurities could be estimated under the same plasma conditions. The estimated decay time of the Si impurities, $\tau_{Si} = 0.12 \pm 0.01$ s, was found to be slightly longer than that of the B impurities, $\tau_B = 0.09 \pm 0.01$ s.

Keywords: TESPEL, impurity transport, neoclassical transport, turbulent transport, Z-dependence

DOI: 10.1585/pfr.16.1202094

The study of the atomic number (Z) dependence of the impurity transport in magnetically confined fusion plasmas is necessary to understand whether turbulent or neoclassical transport is dominant in plasmas. In general, the turbulent-dominant impurity transport does not exhibit a Z-dependence [1]. On the other hand, the neoclassical impurity transport does exhibit such a Z-dependence. An outstanding example of the contribution of the neoclassical transport is the impurity accumulation [2]. Recently, we demonstrated the applicability of the tracer-encapsulated solid pellet (TESPEL) [3] containing a compound tracer for a simultaneous study of the behaviors of different impurities [4]. Following this applicability demonstration, we report here that the simultaneous observation of behaviors of different impurities, which were locally deposited in the core region of the plasma under the same plasma conditions, has been achieved in the Large Helical Device (LHD).

Figure 1 shows the LHD discharge (#169088) waveform summary for this study. The TESPEL (with an outer diameter of 900 μm and a polystyrene (–$CH(C_6H_5)CH_2$–) shell thickness of 120 μm) containing silicon hexaboride (SiB_6) powders was injected at the time of ~ 3.875 s, as indicated by the black vertical dashed line. The target plasma was predominantly heated by tangential NBIs (NBI#2 and NBI#3) but also by perpendicular NBIs (NBI#4 and

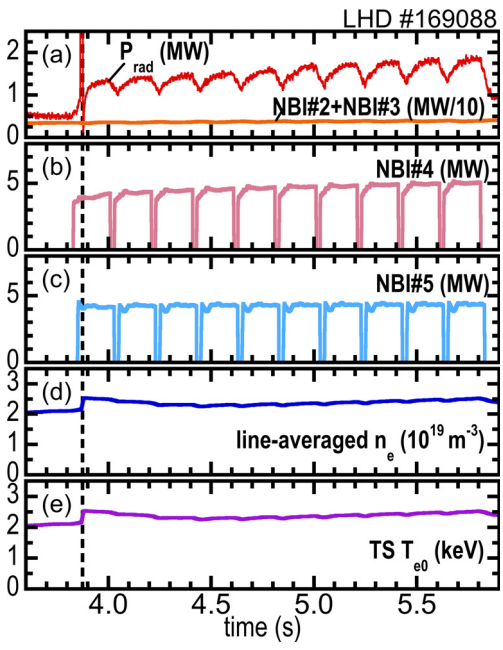

Fig. 1 Temporal evolutions of (a) the plasma radiation power and the tangential NBI power, (b) the perpendicular NBI#4 power, (c) the perpendicular NBI#5 power, (d) the line-averaged electron density, and (e) the central electron temperature. The TESPEL injection time, about 3.875 s, is indicated by a black vertical dashed line.

author's e-mail: tamura.naoki@nifs.ac.jp

NBI#5). Here, the modulated (180 ms on and 20 ms off) NBI#5 was used as a probe beam for the charge-exchange spectroscopy (CXS) diagnostic for the boron (B) measurement. As shown in Fig. 1, the line-averaged electron density, n_{e_bar}, which was about 2×10^{19} m^{-3} before the TESPEL injection, was increased by the TESPEL injection. Subsequently, the increased n_{e_bar} was decreased slightly, without anyhow recovering its pre-injection level. The central electron temperature, T_{e0}, also seemed to be increased by the TESPEL injection. However, since the increment of T_e was observed over a wide range (see Fig. 2 (b). The baseline n_e and T_e profiles, which were measured with a Thomson scattering system [5], are shown in Fig. 2 (a)), this can be explained in terms of the addition of NBI#4 and NBI#5, which were added almost at the same time as the TESPEL injection. The radial profile of the light emissions from the ablating SiB_6-TESPEL is shown in Fig. 2 (f). The dark green line shows the emissions measured with a photomultiplier tube (PMT) through an optical filter with a central wavelength, λ_{center}, of 657.2 nm and a full width half maximum (FWHM) of 1.2 nm; these provide information about Hα (λ = 656.3 nm) from the CH shell. Additionally, the magenta line shows the emissions measured with the PMT through an optical filter with λ_{center} = 412.3 nm and FWHM = 1.1 nm; these provide information about Si II (λ = 413.09 nm) and B II (λ = 412.19 nm) from the SiB_6 tracer. The CH shell ablation was observed in the r_{eff}/a_{99} range from 0.66 to 1.0 (the signal in the r_{eff}/a_{99} range from 0.48 to 0.66 can be considered as the contribution of the continuum radiation). Here, r_{eff} is the averaged minor radius on a magnetic flux surface and a_{99} is the effective minor radius in which 99% of the plasma kinetic energy is confined, which is 0.63 m in this discharge. Furthermore, the emissions from the SiB_6 tracer were observed in the r_{eff}/a_{99} range from 0.48 to 0.74. The difference in the ablation region between the CH shell and the SiB_6 tracer reflects the TESPEL configuration. In this work, r_{eff}/a_{99} = 0 and 1 are considered as the plasma center and boundary, respectively. As shown in Fig. 2 (e), the very high-density region of the B^{5+} ions that appears immediately after the SiB_6-TESPEL injection is in good agreement with the possible deposition region of

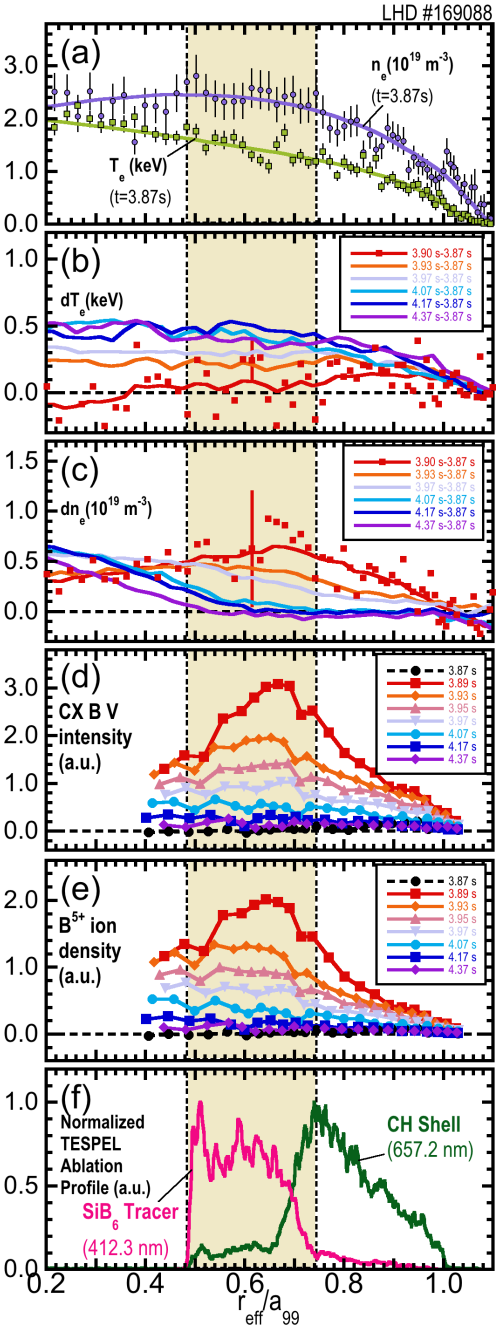

Fig. 2 Radial profiles of (a) the electron density and temperature just before the TESPEL injection, (b) the electron temperature variation, (c) the electron density variation, (d) the CX B V intensity, (e) the B^{5+} ion density, and (f) the normalized TESPEL ablation emissions. The TESPEL injection time is about 3.875 s. A typical error bar is shown in panels (b) and (c).

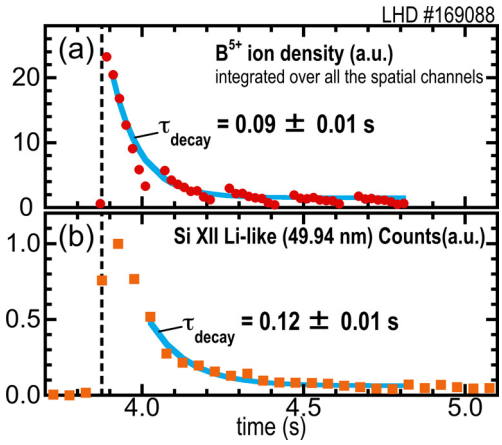

Fig. 3 Decay time estimated for (a) the spatially integrated B^{5+} ion density and (b) the Si XII Li-like emission intensity. The error bars for the data shown are within the size of each symbol.

the SiB_6 tracer. It should be noted here that the pellet ablation profile is not the same as the pellet mass deposition profile. Here, the B^{5+} ion density, $n_B{}^{5+}$, was derived from the charge-exchange line of B V (λ = 494.5 nm, shown in Fig. 2 (d)) and the beam density profile calculated using a beam attenuation code based on the measured n_e and T_e profiles. The hollow profile of $n_B{}^{5+}$ relaxes with time, and the B^{5+} ions eventually disappear from the plasma. The peak position of the $n_B{}^{5+}$ profile seems to move slightly inward. The n_e profile was also changed due to the SiB_6-TESPEL injection (see Fig. 2 (c)). The decay trend of the $n_B{}^{5+}$ profile is a little similar to that of the n_e profile. However, it should be noted here that the n_e increment, especially inside the region with r_{eff}/a_{99} = 0.6, was affected also by NBI fueling. At the same time, Li-like emissions (Si XII, 49.94 nm) from the highly ionized silicon (Si) impurities were also observed with the EUV spectrometer, SOXMOS [6]. Thus, we could estimate the decay times of those impurities under the same plasma conditions. As shown in Fig. 3, the estimated global decay time of the Si impurities, $\tau_{Si} = 0.12 \pm 0.01$ s is slightly longer than that of the B impurities, $\tau_B = 0.09 \pm 0.01$ s. Here, small variations in the temporal behavior of the spatially integrated $n_B{}^{5+}$ in response to the modulation of the perpendicular NBIs are observed. This can be explained in terms of the residual boron resulting from the boronization, etc., but it has a negligible impact on the global decay trend of $n_B{}^{5+}$. These results indicate that the behaviors of impurities with different Z values (Z = 5 and 14) that were locally deposited in the core region of the plasma under the same plasma conditions were successfully obtained.

This work is supported by a JSPS KAKENHI JP19H01881 and the NIFS grant administrative budgets (ULHH007 and ULHH012).

[1] A. Langenberg *et al.*, Phys. Plasmas **27**, 052510 (2020).
[2] N. Tamura *et al.*, Phys. Plasmas **24**, 056118 (2017).
[3] S. Sudo, J. Plasma Fusion Res. **69**, 1349 (1993).
[4] N. Tamura *et al.*, Rev. Sci. Instrum. **92**, 063516 (2021).
[5] I. Yamada *et al.*, JINST **7**, C05007 (2012).
[6] J.L. Schwob *et al.*, Rev. Sci. Instrum. **58**, 1601 (1987).